IOP Publishing Environ. Res. Lett. 19 (2024) 084049 https://doi.org/10.1088/1748-9326/ad5d08

ENVIRONMENTAL RESEARCH
LETTERS

OPEN ACCESS

RECEIVED
26 February 2024

REVISED
10 June 2024

ACCEPTED FOR PUBLICATION
28 June 2024

PUBLISHED
30 July 2024

LETTER

Asynchrony of the seasonal dynamics of gross primary production and ecosystem respiration

Linqing Yang[1,2,3,*] **and Asko Noormets**[3,*]

[1] Wilkes Center for Climate Science and Policy, University of Utah, Salt Lake City, UT 84112, United States of America
[2] School of Biological Sciences, University of Utah, Salt Lake City, UT 84112, United States of America
[3] Department of Ecology and Conservation Biology, Texas A&M University, College Station, TX 77843-2138, United States of America
[*] Authors to whom any correspondence should be addressed.

E-mail: linqingyang_bnu@tamu.edu and noormets@tamu.edu

Keywords: phenology, gross primary production, ecosystem respiration, eddy covariance, carbon sequestration

Supplementary material for this article is available online

Abstract

The phenological cycles of terrestrial ecosystems have shifted with the changing climate, and the altered timings of biogeochemical fluxes may also exert feedback on the climate system. As regulators of land carbon balance, relative shifts in photosynthetic and respiratory phenology under climate change are of great importance. However, the relative seasonal dynamics of these individual processes and their sensitivity to climate factors as well as the implications for carbon cycling are not well understood. In this study, we examined the relationship in the seasonality of gross primary production (GPP) and ecosystem respiration (RE) as well as their temperature sensitivities and the implications for carbon uptake with around 1500 site-years' of data from FLUXNET 2015 and Boreal Ecosystem Productivity Simulator (BEPS) at 212 sites. The results showed that RE started earlier in the spring and ended later in the autumn than GPP over most biomes. Furthermore, the flux phenology metrics responded differently to temperature: GPP phenology was more sensitive to changes during the spring temperature than RE phenology, and less sensitive to autumn temperature than RE. We found large BEPS-observation discrepancies in seasonality metrics and their apparent temperature sensitivity. The site-based BEPS projections did not capture the observed seasonal metrics and temperature sensitivities in either GPP or RE seasonality metrics. Improved understanding of the asynchrony of GPP and RE as well as different sensitivity of environmental factors are of great significance for reliable future carbon balance projections.

1. Introduction

The seasonal dynamics of ecosystem carbon fluxes add to the land surface carbon balance, the interannual variability of which remains a key uncertainty in projecting land-atmosphere relationships under a changing climate (Piao *et al* 2008, Keenan *et al* 2014). The temporal variability in ecosystem net carbon exchange (NEE), including its seasonality, is the result of changing relative contributions of gross primary productivity (GPP) and ecosystem respiration (RE) (Noormets *et al* 2009, Forkel *et al* 2016). The current understanding of each process individually is rather comprehensive across different biomes (Mccree 1974, Farquhar *et al* 1980), while their interplay and subtle differences at longer timescales are not (Duveneck and Thompson 2017). Full understanding of the degree of coordination or asynchrony between GPP and RE, and the factors affecting it, remain important knowledge gaps in global carbon science.

The seasonality of photosynthesis and respiration are often assumed to be synchronous, which has only recently come into question as longer time series measurements of each individual process have become available (Richardson *et al* 2013). Wu *et al* (2012) reported a 'spring lag' between the onset of the growing season of GPP and the onset of the carbon uptake period, and an 'autumn lag' between the end of the growing season of GPP and the end of carbon uptake period. Keenan *et al* (2014) investigated the phenology of GPP and NEE in temperate

forest sites and observed that carbon uptake through photosynthesis increased considerably more than carbon release through respiration for both an earlier spring and later autumn. Both these works indicated the changing proportionality of RE to GPP, but no studies investigated the phenology of GPP and RE directly and individually.

The sensitivity of GPP and RE to different environmental factors may differ (Wu *et al* 2011, Piao *et al* 2013) making predictions of NEE seasonality and its interannual variability inevitably phenomenological, and with limited predictive power (Buitenwerf *et al* 2015). Existing extensive studies demonstrate that temperature is the dominating factor affecting plant phenology, photosynthesis, and respiration (Zhang *et al* 2004, Crous *et al* 2022) and the extension of the growing season in the autumn due to increased warming and delayed freezing can increase annual RE, thus reducing the annual net C uptake (Piao *et al* 2008, Vesala *et al* 2010). Therefore, there is a great need to investigate the phenology of GPP and RE as well as their sensitivity to environmental factors directly and individually.

Here, we analyzed the seasonality metrics of GPP and RE, and their temperature sensitivities and carbon implications, using the flux seasonality metrics generated using GPP and RE fluxes from FLUXNET 2015 dataset and estimates from Boreal Ecosystem Productivity Simulator (BEPS). We asked three questions: (a) Are the seasonality metrics of GPP and RE asynchronous? (b) How are the temperature sensitivities of GPP and RE seasonality? And (c) Whether the seasonality metrics of GPP and RE can affect the accumulated carbon uptake differently?

2. Material and methods

2.1. Data sources and phenology metrics extraction

In this study, we used around 1500 site-years' daily GPP and RE data from FLUXNET 2015 (Pastorello *et al* 2020) and the BEPS at 212 sites (figure 1). BEPS is a process-based prognostic model that simulates global carbon and water cycles, though initially developed for Canadian boreal forest conditions, but has been improved and expanded over regional and global scales (Matsushita and Tamura 2002, Wang *et al* 2003, Schwalm *et al* 2010, Chen *et al* 2019). The input data include meteorological data and N deposition datasets that are the same as those used by the TRENDY models and three LAI time series, GLOBMAP-V2, GLASS, and LAI3g (Chen *et al* 2019). The BEPS was chosen due to it being driven by satellite observations, and its similar or better performance compared to fully prognostic models in simulating the land carbon sink (Chen *et al* 2019, Wang *et al* 2021).

The threshold-based phenology extraction method was used to extract the seasonality metrics for GPP and RE from FLUXNET and BEPS. We first removed the outliers based on a robust outlier exclusion method used in Yang and Noormets (2021) and then fitted the time series data based on a double logistic curve fitting method (equation (1); Gu *et al* 2009, Yang and Noormets 2021, Yang and Liu 2023):

$$f(t) = d + \frac{a_1}{\left(1+e^{-b_1(t-t_1)}\right)^{c_1}} - \frac{a_2}{\left(1+e^{-b_2(t-t_2)}\right)^{c_2}} \quad (1)$$

where $f(t)$ is the eddy-flux data at day of year (DOY) t, d is the background flux, and a_1 and a_2 are parameters about the magnitude. b_1, b_2, c_1 and c_2 are the curvature parameters of transitions.

Then, the start and end of the flux development period (DOY_{SFD}, DOY_{EFD}) in the spring were set at 30% and 70% of the mean amplitude of respective carbon flux for each site-year, which are demonstrated to be commonly used and reliable (Wang *et al* 2019). The start and end of the peak flux period (DOY_{SPF}, DOY_{EPF}) were set at 70% of the mean amplitude. The start and end of the flux recession period (DOY_{SFR}, DOY_{EFR}) were set at 70% and 30% of the mean amplitude. The length of the growing season (L_{AS}) was calculated as the difference between the end of the flux recession period and the start of the flux development period (DOY_{EFR}-DOY_{SFD}). The midpoints of the growing season were set at 50% of the mean amplitude. The seasonality metrics are demonstrated in figure 1.

2.2. Quantification of differences between GPP and RE phenology metrics

We selected four seasonality metrics including DOY_{SFD}, DOY_{EFR}, DOY_{Fmax}, and L_{AS} to compare the asynchrony of GPP and RE using Deming regression. Deming regression acknowledges that the measurement errors in both predictor x and response variable y and the ratio of the error variances are given by $\lambda = \sigma_x^2/\sigma_y^2$ (when the error variances are equal, $\lambda = 1$) (Richardson *et al* 2018). The perpendicular distance d, from each data point to the regression line (intercept b_0, slope b_1) is minimized as in equation (2):

$$d = \frac{(y-(b_0+b_1x))^2}{1+{b_1}^2}. \quad (2)$$

Based on the uncertainties of phenology metrics of GPP and RE (Yang and Noormets 2021), the λ was estimated as 0.75 in this study.

The difference between GPP and RE phenology metrics was calculated as:

$$\text{offset} = \text{Metric}_{RE} - \text{Metrics}_{GPP}. \quad (3)$$

The positive offset values indicate earlier GPP transition dates or longer GPP growing season than

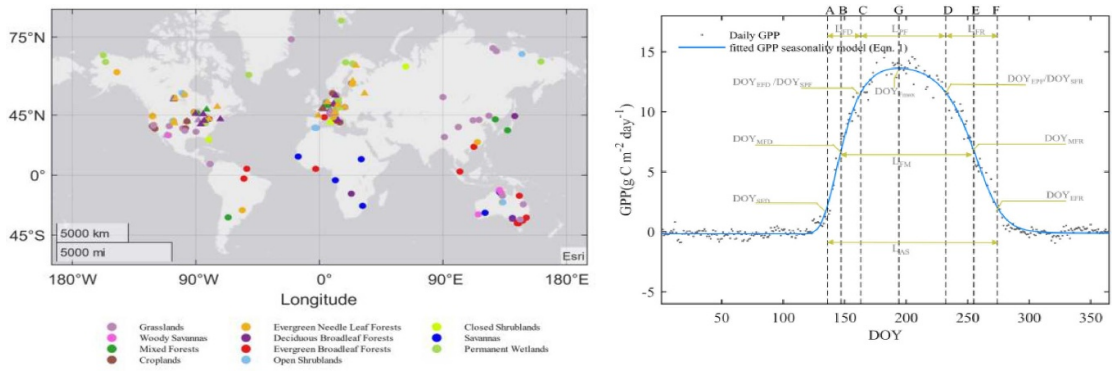

Figure 1. Key seasonality metrics extracted from the global eddy covariance sites. Left: Global distribution of eddy covariance flux sites ($n = 212$) used in this study; color coded by their International Global Biosphere Programme (IGBP) biome type. Triangular marks sites ($n = 48$) with 7 or more years of published data used for the analysis of temporal trends. Right: An example of the seasonal dynamics of gross primary productivity (GPP), and key phenological metrics.

RE and vice versa. Comparison of seasonality metrics among biomes was done with the analysis of variance (ANOVA), and the significance of differences was quantified with Tukey's Honest significant difference post-hoc test, with $\alpha = 0.05$.

2.3. Temperature sensitivities and flux integrals in relation to their phenology metrics

We also analyzed environmental controls including air temperature, soil temperature, vapor pressure deficit, precipitation, soil water content, and shortwave radiation on phenology. The correlation coefficients were then calculated between phenological dates and meteorological variables for the 30 d preceding the mean of the phenology metric. Here, only the eddy covariance sites with at least 7 full years of data were available. This left only 48 sites out of 212, spanning evergreen needle leaf forests (19 sites), deciduous broadleaf forest (DBF) (12 sites), grasslands (8 sites), mixed forests (4 sites), croplands (3 sites), wetlands (2 sites), and woody savannas (1 sites).

The temperature sensitivity of the transition date was calculated as the slope of the relationship between the transition date and the mean air temperature for the 30 d preceding the mean transition date at that site (Keenan *et al* 2014). The temperature sensitivity was defined as:

$$S_T = \frac{\delta P}{\delta T} \tag{4}$$

where δP is the anomaly of a specific phenological transition date, and δT is the anomaly in temperature for the period preceding the mean transition date.

The relationship between the annual and seasonal flux integrals (ΣF_{FD}, ΣF_{PF}, and ΣF_{FR}) with the flux seasonality metrics (L_{FD}, L_{PF} and L_{FR}; figure S2) was evaluated using ordinary least squares regression. Correlation analysis was also performed to examine the contribution of the changes in phenology to interannual variations of carbon flux integrals.

3. Results

3.1. Asynchrony of GPP and RE seasonality

The start, end and length of the growing season (DOY_{SFD}, DOY_{EFR} and L_{AS}, respectively) of both GPP and RE varied. While the overall range of seasonality metrics were similar for GPP and RE (figures 2(A)–(D)), pairwise analysis of the metrics in a given site-year showed that, by and large, they were asynchronous (figures 2(E)–(H)). In spring, GPP started on average 5.9 d later than RE, with the greatest differences in DBFs. $DOY_{SFD\text{-}GPP}$ occurred earlier than $DOY_{SFD\text{-}RE}$ in mixed forest (MF) and evergreen needleleaf forest (ENF), whereas in other biomes such as DBF and croplands (CRO), grasslands (GRA), and savannas (SAV), $DOY_{SFD\text{-}RE}$ preceded $DOY_{SFD\text{-}GPP}$ (figure 2(E)). GPP peaked on average 8.7 d earlier than RE. The difference was consistent in all biomes except in woody savannas (WSA) and DBF (figure 2(F)) and was largest in GRA. In the autumn, RE ended, on average, 16.5 d later than GPP, with the largest (nearly 2 months) difference in CRO and with the exception of WSA. The length of the growing season (L_{AS}) was 22.4 d longer for RE than GPP, with most of that difference occurring in the autumn. However, in ENF $L_{AS\text{-}GPP}$ was 9.5 d longer than $L_{AS\text{-}RE}$ (figure 2(H)), and primarily due to earlier $DOY_{SFD\text{-}RE}$ than $DOY_{SFD\text{-}GEP}$, whereas the season ended at a similar time (figures 2(A) and (D)). In DBF, $L_{AS\text{-}RE}$ were longer than $L_{AS\text{-}GPP}$, due to an earlier spring increase in RE than GPP. The difference between GPP and RE was greatest in L_{FD}, smaller in L_{PF} and smallest (with the notable exceptions of CRO and DBF) in L_{FR} (figure S1). Deviating from other biomes, ENF had a longer $L_{PF\text{-}GPP}$ than $L_{PF\text{-}RE}$, and CRO and DBF had a distinctly longer $L_{FR\text{-}RE}$ than $L_{FR\text{-}GPP}$, while in other biomes they were very similar or $L_{FR\text{-}GPP}$ even exceeded $L_{FR\text{-}RE}$ (figure S1).

The seasonality metrics of GPP and RE simulated by BEPS are more tightly correlated and the offset

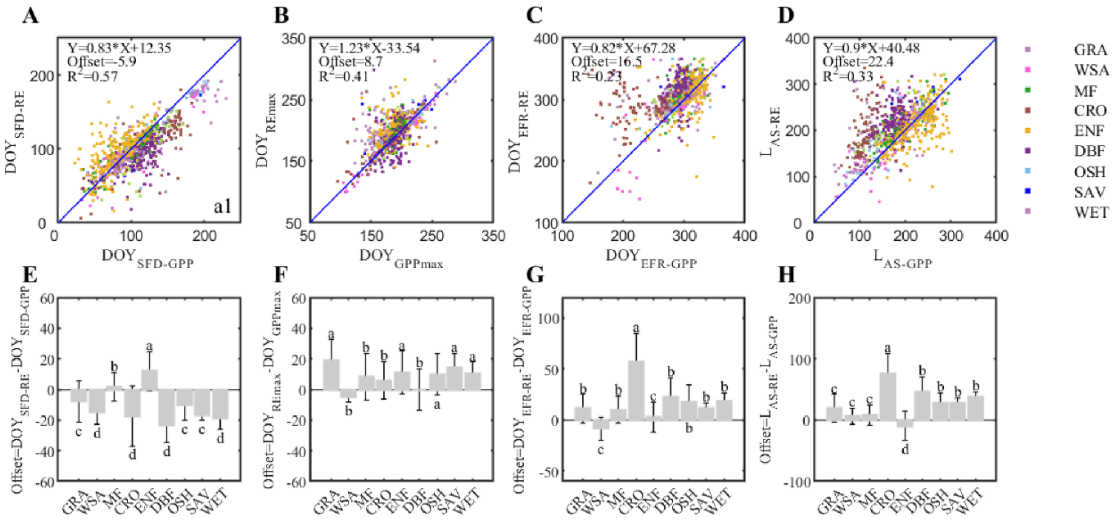

Figure 2. Comparison of the different seasonality metrics of GPP and RE. The 1st row: the scatter plot of different metrics from GPP and RE observations. The 2nd row: Offset between GPP and RE seasonality metrics for 9 different IGBP biomes (mean ± SD). Different letters indicate a statistically significant difference in means ($a = 0.05$). Abbreviations: CRO, cropland; DBF, deciduous broadleaf forest; ENF, evergreen needleleaf forest; GRA, grassland; MF, mixed forest; SAV, savanna; OSH, open shrubland; WET, wetland.

between the respective seasonality metrics are smaller than that observed by eddy covariance data (figure S2). Furthermore, the variability in seasonality metrics observed in eddy covariance was suppressed more in the DOY_{EFR} than in the DOY_{SFD}. We can find that not only the $DOY_{SFD\text{-}GPP}$ and the $DOY_{SFD\text{-}RE}$ are closer and more correlated, but also the offset between them is positive (2.5 d), while that from eddy covariance data is −5.9 d.

3.2. Temperature sensitivities of GPP and RE seasonality

The correlation coefficients between phenology and pre-season environmental factors (air temperature, shortwave radiation, precipitation, vapor pressure deficit, soil temperature, and soil water content preceding the metric of interest; see Methods) were generally higher for DOY_{SFD} than DOY_{EFR} (figure S3). Of the factors examined, Tair exhibited the strongest correlation for both GPP and RE.

On average, a 1 °C increase in Tair advanced $DOY_{SFD\text{-}GPP}$ by 2.38 d and $DOY_{SFD\text{-}RE}$ by 1.75 d (figure 3). The onset of flux recession in the autumn was delayed by 1.17 d per degree in $DOY_{EFR\text{-}GPP}$ and 1.34 d per degree in the $DOY_{EFR\text{-}RE}$. An increase in the summer temperature advanced the timing of peak fluxes by 2.16 d per degree in DOY_{GPPmax} and 2.42 d per degree in DOY_{REmax}. However, the temperature sensitivity of $DOY_{EFR\text{-}RE}$ exhibited contrasting patterns: about a third of sites showed earlier $DOY_{EFR\text{-}RE}$ with increased temperature, whereas the large majority (83.3%) showed later $DOY_{EFR\text{-}GPP}$.

The temperature sensitivity of the timing at the start, end, and peak of the growing seasons did not differ statistically between GPP and RE (figures 3 and 4). Furthermore, the temperature sensitivities showed some divergence among biomes: the contrasts could only be identified as trends that did not always attain statistical significance at the $p < 0.05$ level, given the relatively small sample size ($n = 1$–18). Most notably, the forest biomes and wetlands exhibited positive temperature sensitivity in $DOY_{EFR\text{-}GPP}$ and $DOY_{EFR\text{-}ER}$, whereas the herbaceous biomes (grasslands and crops) exhibited unchanged or earlier at the end of the season. The $DOY_{SFD\text{-}GPP}$ and DOY_{GPPmax} were also marginally more sensitive to interannual temperature anomalies in herbaceous than forest biomes, a trend which was not detected in RE of these small differences between the temperature sensitivities of GPP and RE could be identified as statistically significant.

There is model-observation divergence between the apparent temperature sensitivity of photosynthetic and respiration phenology (figure S5). The BEPS simulated the same sign in the temperature sensitivity of DOY_{SFD} and DOY_{EFR} as observed by eddy covariance, though the magnitude varies. However, the BEPS simulated DOYmax is more temperature sensitive to temperature than observed with eddy covariance.

3.3. Relationships between phenology and carbon fluxes

The integrated fluxes during different phases of the growing season correlated with the timing of the mid-points of these phases (DOY_{MFD} and DOY_{MFR}; figure 4). Longer growing seasons, whether due to earlier spring or later autumn, stimulated both GPP and RE, but the effect was greater on GPP. Earlier $DOY_{MFD\text{-}GPP}$ increased the spring cumulative GPP by 6.69 g C m^{-2} d^{-1} and earlier $DOY_{MFD\text{-}RE}$ increased spring RE by 2.65 g C m^{-2} d^{-1}. Similarly, delayed

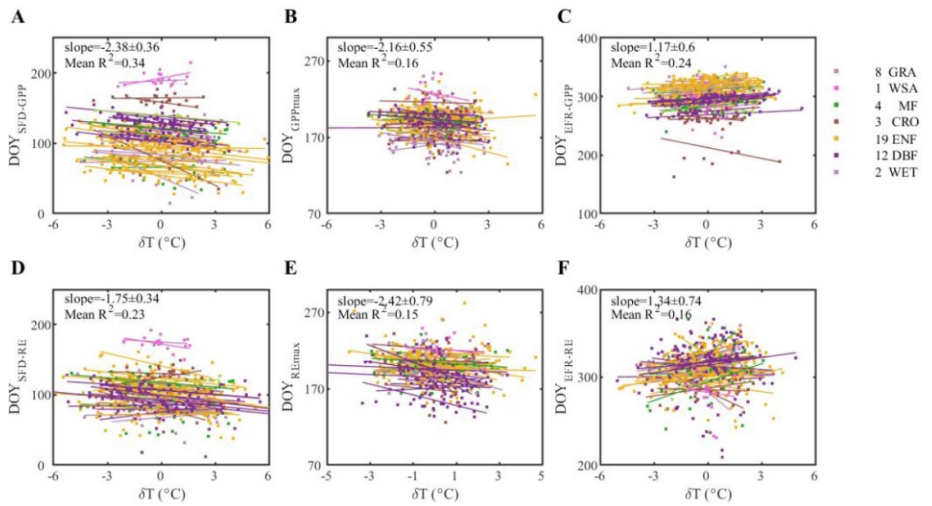

Figure 3. The temperature sensitivity of DOY_{SFD}, DOY_{Fmax}, DOY_{EFR} of GPP and RE from 48 FLUXNET sites, respectively. δT is calculated as the temperature anomaly of one month before the mean phenology date for each site.

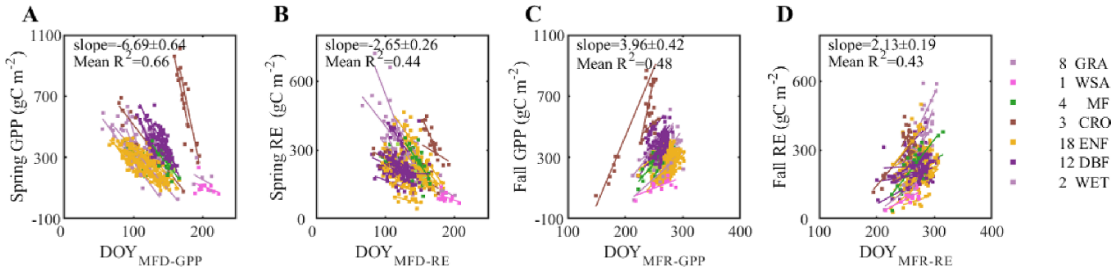

Figure 4. The relationship between midpoints of season dates and integrated seasonal GPP and RE. Dataset includes 48 sites with 7 or more years of data. Spring and autumn are defined as the 60 d intervals centered at the multiyear average DOY_{MFD} and DOY_{MFR} derived from GPP and RE.

$DOY_{MFR\text{-}GPP}$ increased autumn GPP integrals by 3.96 g Cm^{-2} d^{-1} and delayed $DOY_{MFR\text{-}RE}$ RE by 2.13 g C m^{-2} d^{-1}. The combined effect of these changes resulted in greater positive effects on ecosystem net carbon gain (NEP) in the spring than in the autumn.

The length of each of the key phases (flux development period in spring, peak flux period in summer, and the flux recession period in the autumn) also correlated with flux integrals during each of these periods (figure 5). Annual flux integrals of both GPP and RE correlated strongly with the product of peak flux and L_{AS}, and the relationship was stronger for GPP than for RE. The spatial cross-site relationship was similar to the within-site interannual relationship, which works for both GPP and RE. The strong correlations between season length and flux integrals during the corresponding periods can be found, and season length can explain 67%–73% of variance of seasonal flux integrals. In the different periods, this relationship (slope) is different. Furthermore, for GPP, the cross-site relationship within the biomes were similar to within-site relationship, whereas for RE the cross-site relationship within the biomes were slightly more divergent. These relationships among different biomes are generally, statistically not different (figure S6). Notably, the CRO sites had a steeper slope of integrated GPP versus season length which may be due to their human management characteristics.

4. Discussion

4.1. The asynchrony of GPP and RE

The asynchrony between the seasonality metrics of GPP and RE suggests that future changes in these carbon fluxes in response to a warming climate may also be only loosely coupled. This asynchrony was demonstrated in the first comparative analysis of the seasonal dynamics of GPP and RE by Falge *et al* (2002), but not explicitly quantified. Wu *et al* (2012) found both the spring lag and autumn lag between GPP and NEP at 9 DBF and 13 ENF sites across North America and Europe. In this study, we quantified the asynchrony of GPP and RE at 212 global FLUXNET sites, which included more different ecosystems and made the asynchronous discovery more solid and further explored the environmental controls and their carbon uptake implications.

The timing and seasonal offsets of the phenological metrics of GPP and RE differed in a consistent,

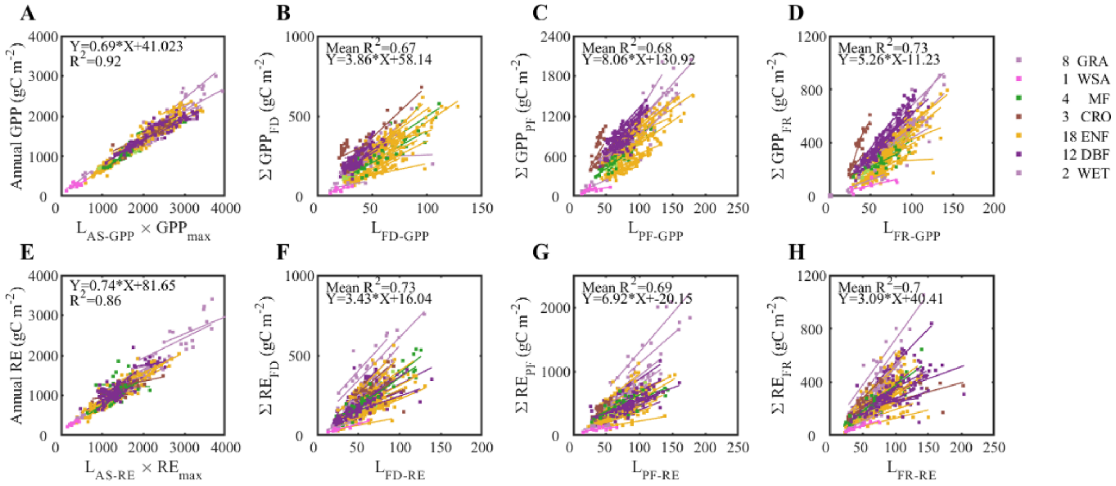

Figure 5. The relationship of accumulated carbon fluxes with length of key duration periods of photosynthetic and respiration phenology. ΣF_{FD}, ΣF_{PF}, and ΣF_{FR} denote accumulated carbon fluxes (GPP and RE) during flux development period, peak flux period, and flux recession period, respectively. Mean R^2 denotes the mean R^2 over all the sites. Dataset includes 48 sites with 7 or more years of data. The number of sites from each biome is indicated in the legend.

yet biome-specific manner. By biome, the differences were large and consistent in wooded ecosystems, especially in ENF and DBF. In DBF and GPP the active season started later than RE in the spring and ended earlier than RE in the autumn. In the spring, DBF requires time to grow new leaves and begin to photosynthesize, while both auto—and heterotrophic respiration begin to ramp up with the rising temperature, with substrate from stored carbohydrates in plants or detritus in the soil (Hopkins *et al* 2013). In the autumn, photosynthesis declines prior to leaf-fall, while heterotrophic respiration may receive a late-season boost from the litter input (Endsley *et al* 2022). In ENF, GPP active season started later in the spring and ended in the autumn at the same time as RE. The ability of ENF to photosynthesize throughout the year when liquid water and light are available is well known (Hu *et al* 2010), while microbial activity in the soil may take longer to ramp up and may slow soil warming compared to deciduous vegetation.

4.2. The temperature sensitivities of GPP and RE seasonality metrics

Our results show that GPP is more sensitive than RE to temperature-driven advances at the start of the growing season (DOY_{SFD}) but less sensitive at the end of the growing season (DOY_{EFR}) (figure S4). Due to the asynchrony between GPP and RE, the mean pre-season temperature of GPP and RE are different in this study, and thus the sensitivities of GPP and RE are based on different phenology dates and temperatures. However, our results are consistent with existing studies (Richardson *et al* 2010, Keenan *et al* 2014): The results that GPP is more sensitive to autumn temperatures than RE in ENF are consistent with Richardson *et al* (2010) and GPP is less sensitive to autumn temperatures than RE in DPFs are consistent with Keenan *et al* (2014). However, the difference in temperature sensitivities of $DOY_{SFD\text{-}GPP}$ and $DOY_{SFD\text{-}RE}$ were not significant, though $DOY_{SFD\text{-}GPP}$ is slightly larger. Earlier studies have attributed the greater temperature sensitivity of DOY_{SFD} than DOY_{EFR} to greater irradiance, and better water availability in spring, and the radiation and carbon sink limitation effects on the autumn phenology (Black *et al* 2000, Kong *et al* 2020, Zani *et al* 2020). It has also been observed that the rate of warming in the spring is greater than that of the rate of cooling in the autumn (Xu *et al* 2013), possibly reflecting the seasonal differences in irradiance. Furthermore, photoperiod decreases the photosynthetic capacity in the autumn by decreasing the maximum Rubisco carboxylation rate and maximum electron transport rate, other than temperature (Bauerle *et al* 2012, Wu *et al* 2021) and increases in the spring and summer productivity advances the autumn phenology, both of which would counteract the warming-induced delays in the autumn phenology (Zani *et al* 2020). The seasonal offsets between GPP and RE may be further exaggerated by the combination of diurnal offsets due to Kok effect (higher temperature-normalized respiration at night than day; Xu *et al* 2013) and phloem loading that transports photoassimilates from mesophyll cells into minor vein phloem sieve tubes (Giaquinta 1977, Sellier and Mammeri 2019), juxtaposed with the greater rate of nighttime than daytime warming (Cox *et al* 2020).

While direct dependence on environmental factors certainly plays a role, sink-strength-dependent allocation of carbon in plants, and the temporally varying surplus of assimilated carbon that can support secondary metabolic pathways, and storage carbohydrate formation, which can be mobilized at times of high metabolic demand (Prescott *et al* 2020) can be important explanations for the temporal decoupling of GPP and RE. Based on first

principles, the dependence on sink strength explains the secondary priority of belowground tissues for carbon for new growth. This perspective assumes passive control of plant carbon allocation, driven by genetic-environmental control of cell division and development, and proximity to a C source. Thus, only when aboveground (especially leaf and apical) growth slows, are assimilated carbohydrates transported preferentially downward, to stem, roots and rhizosymbionts. Such spatially and temporally uneven availability of carbon substrates to different tissues is also consistent with the observations of (i) tight diurnal coupling between respiration and GPP (Mitra *et al* 2019), as well as (ii) their semi-independence (Noormets *et al* 2021).

4.3. Implications

Our phenological observations provide further evidence that the seasonality metrics of GPP and RE are asynchronous and the different temperature sensitivities of GPP and RE seasonality metrics while working on observational and model based GPP and RE individually. Given the increase in global temperatures, phenology-driven increases in carbon uptake may be expected globally. Traditionally, the seasonality of ecosystem carbon balance has been assessed against NEE or GPP seasonality (carbon uptake period, growing season length) (Wu *et al* 2012, Pilegaard and Ibrom 2020, Zhang *et al* 2020), implying temporal stability of RE or near-perfect coupling of RE to GPP. As the data presented clearly does not support this view, we argue that for any predictive capability, these processes must be understood individually, as has been suggested before (Piao *et al* 2008, Kross *et al* 2014, Duveneck and Thompson 2017). Given that the GPP and RE are semi-independent, neither NEE nor GPP dynamics can accurately capture the seasonality of GPP and RE, as well as their asynchronous response to climate factors. This study furthers the understanding and quantifying of the asynchrony and the different responses to warming, however, more work is still needed. For example, whether the findings here still work if expanded to a larger regional or even global scale? To simulate future carbon sink capacity, the models should be updated to allow temporal decoupling of ecosystem respiration and GPP.

Furthermore, the BEPS-simulated GPP and RE seasonality metrics are more tightly correlated and cannot truly affect the asynchrony and temperature sensitivity as observed by eddy covariance (figures S2 and S5), which highlight no consideration of GPP and RE asynchrony in current process models. BEPS is a process-based prognostic model driven by satellite remote sensing products and thus can be expected to have a better performance in capturing the seasonal dynamics of GPP and RE. In BEPS, the timing of onset and senescence of leaf phenology are represented by actual seasonal progression of LAI and the GPP phenology is specially simulated based on a simple multiplicative and threshold formulation of phenology function describing the specific curve rates of photosynthesis phenology with daily mean temperature and day of year as an independent variable, which is used to produce corrected GPP (Gonsamo *et al* 2013). However, more vegetation models are needed to explore and validate and we expect phenology representation in vegetation models needs to improve due to the fact that they do not consider seasonal offsets between GPP and RE (Piao *et al* 2008, Zhang *et al* 2020). One rudimentary method can be incorporating seasonal patterns of eddy covariance based GPP and RE to simulate the carbon uptake phenology. Another method is that we can start with the temperature threshold for photosynthesis and respiration separately and correcting the simulated GPP and RE correspondingly.

Data availability statement

The data that support the findings of this study are openly available at the following URL/DOI: FLUXNET 2015: https://fluxnet.org/data/fluxnet2015-dataset/ and BEPS Modeled GPP and NPP: https://doi.org/10.12199/nesdc.ecodb.2016YFA0600200.02.001 and https://doi.org/10.12199/nesdc.ecodb.2016YFA0600200.02.002.

ORCID iDs

Linqing Yang https://orcid.org/0000-0002-6646-0718
Asko Noormets https://orcid.org/0000-0003-2221-2111

References

Bauerle W L, Oren R, Way D A, Qian S S, Stoy P C, Thornton P E, Bowden J D, Hoffman F M and Reynolds R F 2012 Photoperiodic regulation of the seasonal pattern of photosynthetic capacity and the implications for carbon cycling *Proc. Natl Acad. Sci. USA* **109** 8612–7

Black T A, Chen W J, Barr A G, Arain M A, Chen Z, Nesic Z, Hogg E H, Neumann H H and Yang P C 2000 Increased carbon sequestration by a boreal deciduous forest in years with a warm spring *Geophys. Res. Lett.* **27** 1271–4

Buitenwerf R, Rose L and Higgins S I 2015 Three decades of multi-dimensional change in global leaf phenology *Nat. Clim. Change* **5** 364–8

Chen J M, Ju W, Ciais P, Viovy N, Liu R, Liu Y and Lu X 2019 Vegetation structural change since 1981 significantly enhanced the terrestrial carbon sink *Nat. Commun.* **10** 4259

Cox D T C, Maclean I M D, Gardner A S and Gaston K J 2020 Global variation in diurnal asymmetry in temperature, cloud cover, specific humidity and precipitation and its association with leaf area index *Glob. Change Biol.* **26** 7099–111

Crous K Y, Uddling J, Kauwe D E and G M 2022 Temperature responses of photosynthesis and respiration in evergreen trees from boreal to tropical latitudes *New Phytol.* **234** 353–74

Duveneck M J and Thompson J R 2017 Climate change imposes phenological trade-offs on forest net primary productivity *J. Geophys. Res.* **122** 2298–313

Endsley K A, Kimball J S and Reichle R H 2022 Soil respiration phenology improves modeled phase of terrestrial net ecosystem exchange in northern hemisphere *J. Adv. Model. Earth Syst.* **14** e2021MS002804

Falge E *et al* 2002 Seasonality of ecosystem respiration and gross primary production as derived from FLUXNET measurements *Agric. For. Meteorol.* **113** 53–74

Farquhar G D, Von Caemmerer S and Berry J A 1980 A biochemical model of photosynthetic CO2 assimilation in leaves of C 3 species *Planta* **149** 78–90

Forkel M, Carvalhais N, Rodenbeck C, Keeling R, Heimann M, Thonicke K, Zaehle S and Reichstein M 2016 Enhanced seasonal CO2 exchange caused by amplified plant productivity in northern ecosystems *Science* **351** 696–9

Giaquinta R 1977 Sucrose hydrolysis in relation to phloem translocation in beta vulgaris *Plant Physiol.* **60** 339–43

Gonsamo A, Chen J M and D'odorico P 2013 Deriving land surface phenology indicators from CO2 eddy covariance measurements *Ecol. Indicators* **29** 203–7

GU L, Post W M, Baldocchi D D, Black T A, Suyker A E, Verma S B, Vesala T and Wofsy S C 2009 Characterizing the seasonal dynamics of plant community photosynthesis across a range of vegetation types *Phenology of Ecosystem Processes* (Springer) (https://doi.org/10.1007/978-1-4419-0026-5_2)

Hopkins F, Gonzalez-Meler M A, Flower C E, Lynch D J, Czimczik C, Tang J and Subke J A 2013 Ecosystem-level controls on root-rhizosphere respiration *New Phytol.* **199** 339–51

Hu J I A, Moore D J P, Burns S P and Monson R K 2010 Longer growing seasons lead to less carbon sequestration by a subalpine forest *Glob. Change Biol.* **16** 771–83

Keenan T F *et al* 2014 Net carbon uptake has increased through warming-induced changes in temperate forest phenology *Nat. Clim. Change* **4** 598–604

Kong D, Zhang Y, Wang D, Chen J and GU X 2020 Photoperiod explains the asynchronization between vegetation carbon phenology and vegetation greenness phenology *J. Geophys. Res.* **125** e2020JG005636

Kross A S E, Roulet N T, Moore T R, Lafleur P M, Humphreys E R, Seaquist J W, Flanagan L B and Aurela M 2014 Phenology and its role in carbon dioxide exchange processes in northern peatlands *J. Geophys. Res.* **119** 1370–84

Matsushita B and Tamura M 2002 Integrating remotely sensed data with an ecosystem model to estimate net primary productivity in East Asia *Remote Sens. Environ.* **81** 58–66

Mccree K J 1974 Equations for the rate of dark respiration of white clover and grain sorghum, as functions of dry weight, photosynthetic rate, and temperature *Crop Sci.* **14** 509–14

Mitra B, Miao G, Minick K, Mcnulty S G, Sun G, Gavazzi M, King J S and Noormets A 2019 Disentangling the effects of temperature, moisture, and substrate availability on soil CO_2 efflux *J. Geophys. Res.* **124** 2060–75

Noormets A *et al* 2021 Heterotrophic respiration and the divergence of productivity and carbon sequestration *Geophys. Res. Lett.* **48** e2020GL092366

Noormets A, Chen J, GU L and Desai A 2009 The phenology of gross ecosystem productivity and ecosystem respiration in temperate hardwood and conifer chronosequences *Phenology of Ecosystem Processes* (Springer) (https://doi.org/10.1007/978-1-4419-0026-5_3)

Pastorello G, Trotta C, Ribeca A, Elbashandy A, Barr A and Papale D 2020 The FLUXNET2015 dataset and the ONEFlux processing pipeline for eddy covariance data **7** 250

Piao S *et al* 2008 Net carbon dioxide losses of northern ecosystems in response to autumn warming *Nature* **451** 49–52

Piao S *et al* 2013 Evaluation of terrestrial carbon cycle models for their response to climate variability and to CO_2 trends *Glob. Change Biol.* **19** 2117–32

Pilegaard K and Ibrom A 2020 Net carbon ecosystem exchange during 24 years in the Sorø Beech Forest—relations to phenology and climate *Tellus* B **72** 1–17

Prescott C E, Grayston S J, Helmisaari H S, Kastovska E, Korner C, Lambers H, Meier I C, Millard P and Ostonen I 2020 Surplus Carbon Drives Allocation and Plant-Soil Interactions *Trends Ecol. Evol.* **35** 1110–8

Richardson A D *et al* 2010 Influence of spring and autumn phenological transitions on forest ecosystem productivity *Phil. Trans. R. Soc.* B **365** 3227–46

Richardson A D, Hufkens K, Milliman T and Frolking S 2018 Intercomparison of phenological transition dates derived from the PhenoCam Dataset V1.0 and Modis satellite remote sensing *Sci. Rep.* **8** 5679

Richardson A D, Keenan T F, Migliavacca M, Ryu Y, Sonnentag O and Toomey M 2013 Climate change, phenology, and phenological control of vegetation feedbacks to the climate system *Agric. For. Meteorol.* **169** 156–73

Schwalm C R *et al* 2010 A model-data intercomparison of CO_2 exchange across North America: results from the North American Carbon Program site synthesis *J. Geophys. Res.* **115** G00H05

Sellier D and Mammeri Y 2019 Diurnal dynamics of phloem loading: theoretical consequences for transport efficiency and flow characteristics *Tree Physiol.* **39** 300–11

Vesala T *et al* 2010 Autumn temperature and carbon balance of a boreal Scots pine forest in Southern Finland *Biogeosciences* **7** 163–76

Wang M, Wang S, Zhao J, Ju W and Hao Z 2021 Global positive gross primary productivity extremes and climate contributions during 1982–2016 *Sci. Total Environ.* **774** 145703

Wang Q, Tenhunen J, Falge E, Bernhofer C, Granier A and Vesala T 2003 Simulation and scaling of temporal variation in gross primary production for coniferous and deciduous temperate forests *Glob. Change Biol.* **10** 37–51

Wang X, Xiao J, LI X, Cheng G, MA M, Zhu G, Altaf Arain M, Andrew Black T and Jassal R S 2019 No trends in spring and autumn phenology during the global warming hiatus *Nat. Commun.* **10** 2389

Wu C, Chen J M, Gonsamo A, Price D T, Black T A and Kurz W A 2012 Interannual variability of net carbon exchange is related to the lag between the end-dates of net carbon uptake and photosynthesis: evidence from long records at two contrasting forest stands *Agric. For. Meteorol.* **164** 29–38

Wu Z, Chen S, De Boeck H J, Stenseth N C, Tang J, Vitasse Y, Wang S, Zohner C and Fu Y H 2021 Atmospheric brightening counteracts warming-induced delays in autumn phenology of temperate trees in Europe *Glob. Ecol. Biogeogr.* **30** 2477–87

Wu Z, Dijkstra P, Koch G W, Peñuelas J and Hungate B A 2011 Responses of terrestrial ecosystems to temperature and precipitation change: a meta-analysis of experimental manipulation *Glob. Change Biol.* **17** 927–42

Xu L *et al* 2013 Temperature and vegetation seasonality diminishment over northern lands *Nat. Clim. Change* **3** 581–6

Yang L and Liu M 2023 2021 February texas ice storm induced spring GPP reduction compensated by the higher precipitation *Earth's Future* **11**

Yang L and Noormets A 2021 Standardized flux seasonality metrics: a companion dataset for Fluxnet annual product *Earth Syst. Sci. Data* **13** 1461–75

Zani D, Crowther T W, MO L, Renner S S and Zohner C M 2020 Increased growing-season productivity drives earlier autumn leaf senescence in temperate trees *Science* **370** 1066–71

Zhang X, Friedl M A, Schaaf C B and Strahler A H 2004 Climate controls on vegetation phenological patterns in northern mid- and high latitudes inferred from Modis data *Glob. Change Biol.* **10** 1133–45

Zhang Y, Commane R, Zhou S, Williams A P and Gentine P 2020 Light limitation regulates the response of autumn terrestrial carbon uptake to warming *Nat. Clim. Change* **10** 739–43